



ELSEVIER

Journal of Alloys and Compounds 323–324 (2001) 736–739

Journal of  
ALLOYS  
AND COMPOUNDS

www.elsevier.com/locate/jallcom

# Infra-red-to-visible wavelength upconversion in $\text{Sm}^{3+}$ -activated YAG crystals

M. Kaczkan<sup>a,\*</sup>, Z. Frukacz<sup>b</sup>, M. Malinowski<sup>a</sup><sup>a</sup>*Institute of Microelectronics and Optoelectronics PW, ul. Koszykowa 75, 00-662 Warsaw, Poland*<sup>b</sup>*Institute of Electronic Materials Technology, ul. Wólczyńska 133, 01-919 Warsaw, Poland*

## Abstract

Upconverted green–yellow emission has been generated at room temperature in  $\text{Y}_3\text{Al}_5\text{O}_{12}:\text{Sm}^{3+}$  crystals after pulsed 925–950 nm infra-red excitation. The dynamics of the involved excited states were analyzed under pulsed laser excitation. The upconversion mechanisms were investigated and shown to be quasi-resonant energy transfers. © 2001 Elsevier Science B.V. All rights reserved.

*Keywords:* Insulators; Electronic states; Optical properties; Luminescence; Time-resolved optical spectroscopies

## 1. Introduction

The emission spectrum of trivalent samarium ( $\text{Sm}^{3+}$ ) is dominated by transitions from the  $^4\text{G}_{5/2}$  excited state located at about  $17\,500\text{ cm}^{-1}$  [1]. Due to the large energy gap of about  $7000\text{ cm}^{-1}$  to the next lower level, the  $^4\text{G}_{5/2}$  decay is predominantly radiative. The strongest emission is observed in the red part of the spectrum. Laser action in  $\text{Sm}^{3+}$ -activated solids has only been reported, to our knowledge, in  $\text{TbF}_3:\text{Sm}^{3+}$  [2] and  $\text{LiTbF}_4:\text{Sm}^{3+}$  [3] crystals and  $\text{Sm}^{3+}$ -doped silica glass fiber [4]. Moreover, in silica fiber devices, fast optical switching [5] and gain equalization for an erbium amplifier [6] have been realized. Recently,  $\text{YAG}:\text{Sm}^{3+}$  has been of interest in the static ultrahigh pressure research area as an optical pressure sensor [7,8]. However, very little is known about the spectroscopy of  $\text{Sm}^{3+}$ -activated  $\text{Y}_3\text{Al}_5\text{O}_{12}$  (YAG) crystals; the room temperature absorption spectrum of this material has been presented in Ref. [9] and some of the low-lying energy level values were given in Ref. [10]. In an earlier paper [11] we reported an investigation of the emission properties of  $\text{Sm}^{3+}$  in YAG; the energy level diagram was established, the emission characteristics of the  $^4\text{G}_{5/2}$  metastable state were determined and the oscillator strengths of various  $\text{Sm}^{3+}$  transitions were investigated using Judd–Ofelt theory.

In this work, the first observation of upconversion

fluorescence from the  $^4\text{G}_{5/2}$  level of  $\text{YAG}:\text{Sm}^{3+}$  induced by pumping in the 925–950 nm range is reported. As the upconversion phenomena in rare-earth-doped systems are useful for developing efficient short-wavelength solid-state lasers [12,13], several processes of this type, including sequential two-photon or multiphoton absorption, energy transfer, and avalanche absorption, have been intensively studied in bulk and waveguide materials activated with  $\text{Pr}^{3+}$ ,  $\text{Nd}^{3+}$ ,  $\text{Er}^{3+}$ ,  $\text{Tm}^{3+}$  and  $\text{Ho}^{3+}$ . To our knowledge, upconversion for  $\text{Sm}^{3+}$  has only been reported in low phonon hosts such as  $\text{GdOCl}$  [14] and  $\text{LaBr}_3$  [15]. The purpose of this investigation was to study the upconversion properties of a  $\text{YAG}:\text{Sm}^{3+}$  crystal to develop a better general understanding of the behavior of  $\text{Sm}^{3+}$  in this host and to predict its potential laser properties.

## 2. Results and discussion

Two  $\text{YAG}:\text{Sm}^{3+}$  samples with activator concentrations of 0.1 and 0.5 at% were grown using the Czochralski technique at the ITME Laboratory in Warsaw. Luminescence was excited by a cw Carl Zeiss ILA 120 argon laser or tunable optical parametric oscillator (Continuum) pumped by a frequency-tripled  $\text{YAG}:\text{Nd}$  pulse laser (Continuum Surelite II). The emission signal from the sample was dispersed by a GDM 1000 monochromator and detected by an EMI 9789 cooled GaAs photomultiplier. Data acquisition was performed using a Stanford SR 400 photon-counting system controlled by a PC. Luminescence lifetime measurements were carried out using a Stanford

\*Corresponding author. Tel.: +48-22-660-5047; fax: +48-22-628-8740.

E-mail address: kaczkan@imio.pw.edu.pl (M. Kaczkan).

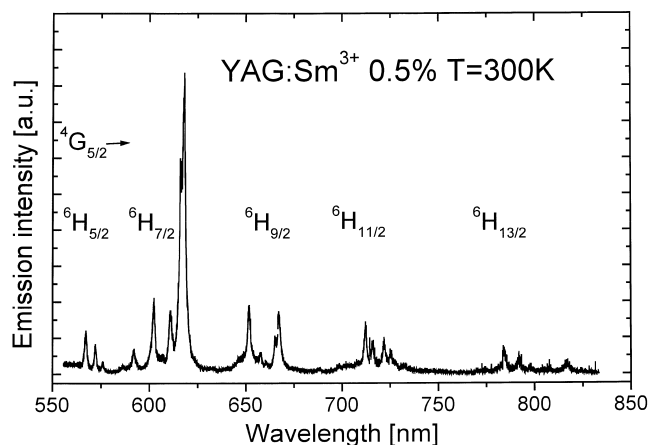


Fig. 1. Room temperature emission spectrum of a 0.5%  $\text{Sm}^{3+}$ -doped YAG crystal resulting from 476 nm excitation.

SR 430 multichannel analyzer. For low-temperature measurements, a Displex Model CSW-202 closed cycle cryogenic system was used.

Green emission and several transitions in the visible part of the spectrum, characteristic for the  ${}^4\text{G}_{5/2}$  emission of samarium, were observed at 300 K for an excitation wavelength in the 925–950 nm band. Fig. 1 presents the room temperature emission spectrum obtained by 476 nm excitation. The strongest luminescence was in the 617 nm band and was assigned to the  ${}^4\text{G}_{5/2} \rightarrow {}^6\text{H}_{7/2}$  transition. The excitation spectrum of this anti-Stokes fluorescence measured in  $\text{YAG}:\text{Sm}^{3+}$  is presented in Fig. 2.

The decay profile of the 617 nm emission resulting from IR excitation at 941.5 nm ( $10\,622\text{ cm}^{-1}$ ) is shown in Fig. 3. For comparison, direct one-photon (OP) excited decay is also presented in the same figure. It can be seen that IR excited decay is exponential with a lifetime of 2 ms and no observable rise-time, as after direct OP excitation. Finally,

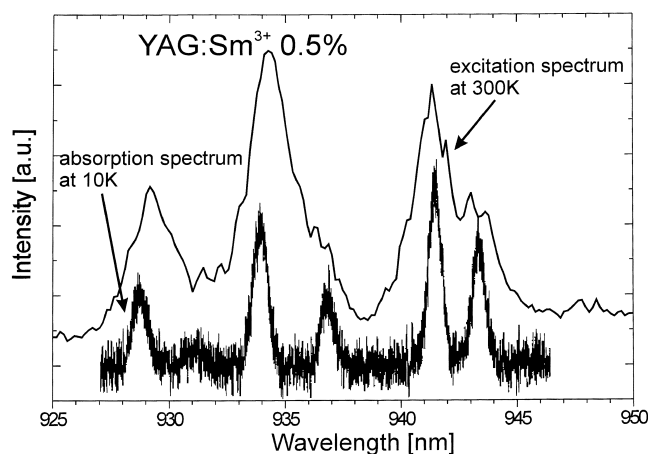


Fig. 2. Infra-red excitation spectrum of the upconversion  ${}^4\text{G}_{5/2}$  emission at 617 nm and (bottom) the low temperature absorption spectrum corresponding to the ground state  ${}^6\text{H}_{5/2} \rightarrow {}^6\text{F}_{11/2}$  absorption in  $\text{YAG}:\text{Sm}^{3+}$ .

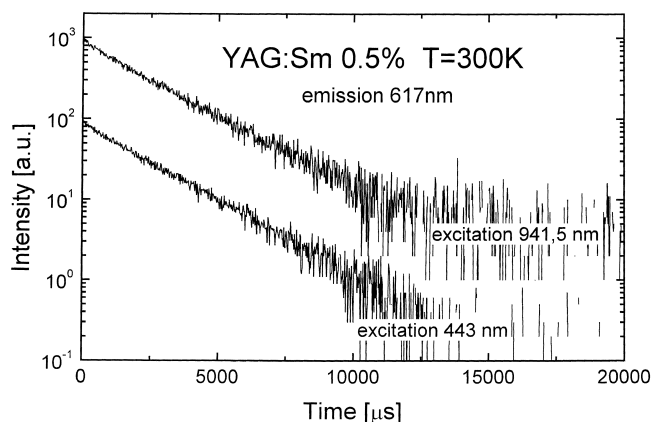


Fig. 3. Decay profile of the upconverted  ${}^4\text{G}_{5/2} \rightarrow {}^6\text{H}_{7/2}$  (617 nm) luminescence in  $\text{YAG}:\text{Sm}^{3+}$  resulting from IR (941.5 nm) pumping at 300 K.

a square intensity dependence of the upconverted  ${}^4\text{G}_{5/2}$  emission on IR excitation was determined, and is presented in Fig. 4.

The two-photon character of the observed upconversion process is confirmed by its square intensity dependence. The absence of a rise time and the lack of any lifetime changes with respect to OP excited decay is typical for an ESA process. However, from Fig. 2 it can be seen that both excitation and absorption spectra have the same form and that the upconversion excitation wavelengths correspond to absorption of the  ${}^6\text{F}_{11/2}$  multiplet of  $\text{YAG}:\text{Sm}^{3+}$  [11]. Thus, it can be concluded that the pulsed upconversion is due to energy transfer upconversion (ETU). From the energy level diagram, several resonant processes of this type can be suggested. Infra-red-to-green light upconversion transitions, possible at room temperature, are shown in Fig. 5. One of the two coupled  $\text{Sm}^{3+}$  ions, simultaneously excited through the ground state absorption by infra-red photons to the  ${}^6\text{F}_{11/2}$  state, transfers its energy to the neighboring ion leaving it in the higher excited state from which anti-Stokes emission can be observed. It was also observed that, at low temperatures, the efficiency of

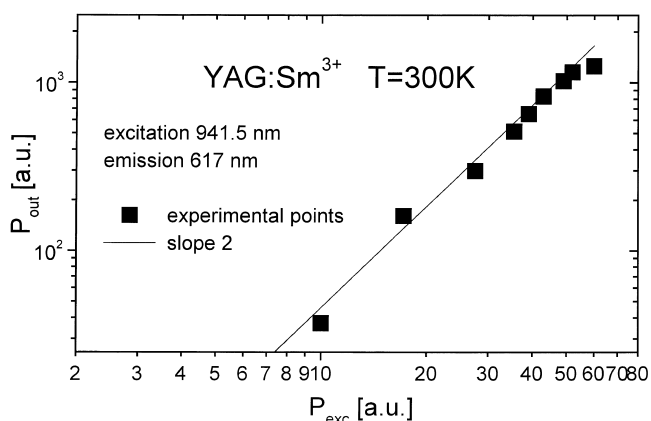


Fig. 4. Variation of the upconverted  ${}^4\text{G}_{5/2}$  luminescence with IR excitation intensity at  $\lambda = 941.5\text{ nm}$  at 300 K. (—) Square dependence.

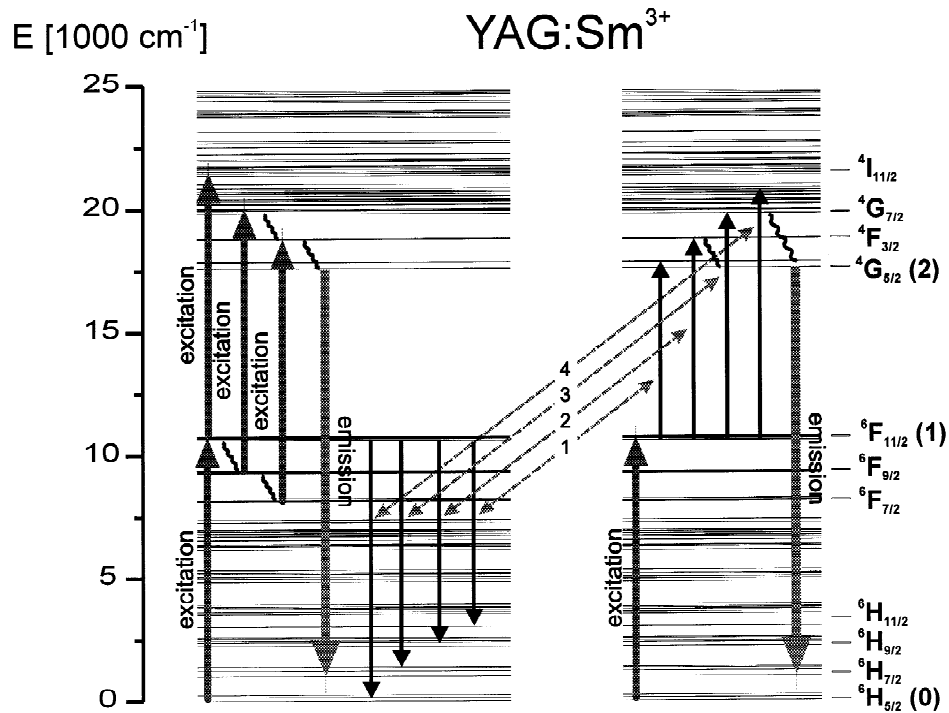


Fig. 5. Simplified energy-level diagram for YAG:Sm<sup>3+</sup> explaining upconversion excitation transitions.

the upconversion process was much less than at 300 K, indicating its non-resonant, phonon-assisted character or thermal activation by the population of higher Stark levels in the ground and excited states. Analysis of the collected data leads to quasi-resonant upconversion transitions of the type

$$\begin{aligned} & {}^6F_{11/2}(10\ 600\ \text{cm}^{-1}) \rightarrow {}^6H_{5/2}(0) \\ & = {}^6F_{11/2}(10\ 600\ \text{cm}^{-1}) \rightarrow {}^4I_{11/2}(21\ 374\ \text{cm}^{-1}) \\ & \quad - 174\ \text{cm}^{-1} \end{aligned}$$

$$\begin{aligned} & {}^6F_{11/2}(10\ 600\ \text{cm}^{-1}) \rightarrow {}^6H_{7/2}(1012\ \text{cm}^{-1}) \\ & = {}^6F_{11/2}(10\ 600\ \text{cm}^{-1}) \rightarrow {}^4I_{9/2}(20\ 202\ \text{cm}^{-1}) - 14\ \text{cm}^{-1} \end{aligned}$$

$$\begin{aligned} & {}^6F_{11/2}(10\ 600\ \text{cm}^{-1}) \rightarrow {}^6H_{9/2}(2401\ \text{cm}^{-1}) \\ & = {}^6F_{11/2}(10\ 600\ \text{cm}^{-1}) \rightarrow {}^4F_{3/2}(18\ 794\ \text{cm}^{-1}) + 5\ \text{cm}^{-1} \end{aligned}$$

$$\begin{aligned} & {}^6F_{11/2}(10\ 600\ \text{cm}^{-1}) \rightarrow {}^6H_{11/2}(3559\ \text{cm}^{-1}) \\ & = {}^6F_{11/2}(10\ 600\ \text{cm}^{-1}) \rightarrow {}^4G_{5/2}(17\ 601\ \text{cm}^{-1}) + 40\ \text{cm}^{-1} \end{aligned}$$

$$\begin{aligned} & {}^6F_{11/2}(10\ 600\ \text{cm}^{-1}) \rightarrow {}^6H_{11/2}(3642\ \text{cm}^{-1}) \\ & = {}^6F_{11/2}(10\ 600\ \text{cm}^{-1}) \rightarrow {}^4G_{5/2}(17\ 601\ \text{cm}^{-1}) - 43\ \text{cm}^{-1} \end{aligned}$$

By solving the population equations for the doubly excited ion pair in the  ${}^4G_{5/2}$  state -2 (see also Fig. 5):

$$\dot{N}_1 = R_{01}N_0 - 2W_T N_1^2 - \frac{N_1}{\tau_1}$$

$$\dot{N}_2 = W_T N_1^2 - \frac{N_2}{\tau_2}$$

and assuming that the  ${}^6H_{5/2} \rightarrow {}^6F_{11/2}$  pumping rate  $R_{01}$  is much higher than the decay rate of the  ${}^4G_{5/2}$  and  ${}^6F_{11/2}$  states,  $R_{01} \gg 1/\tau_2, 1/\tau_1$  and that  $\tau_2 \gg \tau_1$ , the time evolution of the upconverted signal can be written as

$$N_2(t) = \frac{k\tau_1}{2} \exp(-t/\tau_2) \quad (1)$$

where

$$k = \frac{W_T N_1^2(0)}{\tau_1^2 (1/\tau_1 + 2W_T N_1(0))^2} \neq f(t) \text{ for } t \gg \tau_2$$

and  $W_T$  is the energy transfer rate. The assumption was made that we are concerned with weakly interacting pairs and that the transfer rates involved are smaller than the radiative relaxation rates. It can be seen that, according to Eq. (1) and due to the very short lifetime of the  ${}^6F_{11/2}$  state, the decay of the  ${}^4G_{5/2}$  upconverted signal is governed by the intrinsic decay time of this state, which was observed during our experiments.

ESA transitions from the  ${}^6F_{11/2}$  level of samarium are not likely to occur because of the short lifetime of this state, which, from the energy gap law for YAG [16], was evaluated to be of the order of 10 ns. Using the Judd-Ofelt [17,18] formalism and the intensity parameters calculated previously [11] the cross-section values for these ESA transitions were determined. Table 1 shows the calculated ground state absorption (GSA) and ESA cross sections

Table 1

Ground state absorption (GSA) and excited state absorption (ESA) cross sections,  $\sigma$ , calculated for YAG:Sm<sup>3+</sup> together with the corresponding matrix elements for the considered transitions

	Transition	Matrix elements			$\sigma$ (cm <sup>2</sup> )
		$U_2^2$	$U_4^2$	$U_6^2$	
GSA	${}^6H_{5/2} \rightarrow {}^6F_{11/2}$	0	0.0010	0.0520	$1.80 \times 10^{-20}$
ESA	${}^6F_{11/2} \rightarrow {}^4I_{11/2}$	0	0.0008	0.0033	$1.40 \times 10^{-21}$
	${}^6F_{9/2} \rightarrow {}^4G_{7/2}$	0.0004	0	0.0006	$2.94 \times 10^{-22}$
	${}^6F_{7/2} \rightarrow {}^4F_{3/2}$	0	0.0013	0	$5.26 \times 10^{-22}$

together with the corresponding matrix elements for the considered transitions. It can be seen that the  $\sigma_{\text{ESA}}$  values are about two orders of magnitude lower than the  $\sigma_{\text{GSA}}$  values, indicating that, despite the short lifetime of the metastable  ${}^6F_{11/2}$  state, this process is not expected to be efficient.

### 3. Conclusion

In summary, the process of upconversion leading to the green  ${}^4G_{5/2}$  emission of Sm<sup>3+</sup> has been studied for the first time in an oxide host–YAG crystal. The most probable mechanism is quasi-resonant energy transfer between two Sm<sup>3+</sup> ions.

### References

[1] G.H. Dieke, Spectra and Energy Levels of Rare-earth Ions in Crystals, Interscience, New York, 1968.

- [2] B.N. Kazakov, M.S. Orlov, M.V. Petrov, A.L. Stolov, A.M. Tkachuk, Opt. Spectrosc. (USSR) 47 (1979) 676.
- [3] H.P. Janssen, Advanced Solid State Lasers Technical Digest, ME2-1/73, Memphis, 1995.
- [4] M.C. Farries, P.R. Morkel, J.E. Townsend, Electron. Lett. 24 (1988) 709.
- [5] B. Wu, P.L. Chu, IEEE Photon Technol. Lett. 8 (1996) 230.
- [6] S.K. Liaw, Y.K. Chen, IEEE Photon Technol. Lett. 8 (1996) 879.
- [7] N.J. Hess, D. Schiferl, J. Appl. Phys. 71 (1992) 2082.
- [8] J. Liu, Y.K. Vohra, Appl. Phys. Lett. 64 (1994) 3386.
- [9] M.J. Weber (Ed.), Lasers and Masers, CRC Handbook of Laser Science and Technology, Vol. I, CRC Press, Boca Raton, FL, 1982, p. 29.
- [10] P. Grunberg, Z. Phys. 225 (1969) 376.
- [11] M. Malinowski, R. Wolski, Z. Frukacz, T. Lukasiewicz, Z. Luczynski, J. Appl. Spectrosc. 62 (1995) 49.
- [12] A.J. Silversmith, W. Lenth, R.M. Macfarlane, Appl. Phys. Lett. 51 (1987) 1977.
- [13] P. Xie, T.R. Gosnell, Opt. Lett. 20 (1995) 1014.
- [14] S. Areva, J. Holsa, R.-J. Lamminmaki, H. Rahiala, P. Deren, W. Strek, in: Third International Winter Workshop RES'99, Szklarska Poreba, Poland, 27 April, 1999, p. 67.
- [15] T. Riedener, H.U. Gudel, in: International Conference Lumin ICL'96, Prague, August, 1996, p. 14.
- [16] R. Raisfeld, C.K. Jorgensen, Lasers and Excited States of Rare-earth, Springer, Heidelberg, 1977.
- [17] B.R. Judd, Phys. Rev. 127 (1962) 750.
- [18] G.S. Ofelt, J. Chem. Phys. 37 (1962) 511.